ELECTRICALLY ISOLATED SYSTEM RESPONSE TO RAPID CHARGING EVENTS USING HOLLOW CATHODE NEUTRALIZATION

Grant Miars[(1)], Omar Leon[(2)], Brian Gilchrist[(1)], Gian Luca Delzanno[(3)], Joe Borovsky[(4)]

[(1)]*Department of Electrical Engineering, University of Michigan, 1303 Beal Ave., 2240 EECS, Ann Arbor, MI, 48109, USA, Email: gmiars@umich.edu & gilchrst@umich.edu*

[(2)] *Applied Physics Program, University of Michigan, 450 Church St., 1425 Randall, Ann Arbor, MI, 48109, USA, Email: omarleon@umich.edu*

[(3)]*Los Alamos National Laboratory, Mail stop: K717, Los Alamos, NM, 87545, USA, Email: delzanno@lanl.gov*

[(4)]*CLASP, University of Michigan, 2455 Hayward St., Ann Arbor, MI, USA, Email: jborovsky@spacescience.org*

ABSTRACT

Experiments were performed in the 6m x 9m Large Vacuum Test Facility (LVTF) at the Plasmadynamics and Electric Propulsion Laboratory (PEPL) to determine the efficacy and key parameters of a hollow cathode based neutralization technique for a spacecraft in the Magnetosphere. The laboratory electrical isolation circuit described here approximates aspects of this in-space "spacecraft" environment. "Spacecraft" potential is presented for transient and steady state conditions for various representative "beam" currents while operating the hollow cathode. Hollow cathode parameters are varied to determine their effect on neutralization efficiency. Keeper discharge current and ionization fraction are found to be the key cathode parameters as suggested via theory/simulation. "Spacecraft" potential transients occur over the course of a few seconds, far exceeding the characteristic reaction time of the plasma by itself. Possible system-based explanations for these long transients are presented. The presence of microdischarges within the chamber is examined for high "spacecraft" and plasma potentials.

1. INTRODUCTION

There is significant interest within the atmospheric science community to map the magnetic field lines of the Earth in real time [1]. A mission has been proposed to map these fields through high power electron beam emission in the magnetosphere which will follow field lines and be visibly dissipated in the Earth's lower atmosphere. Electron beams have been used for similar purposes on board sounding rockets and satellites in Low Earth Orbit (LEO) in the past [2]. Sufficient return current to neutralize the spacecraft has been easily achieved in these regions as the plasma density is nominally 10^5cm^{-3}. In comparison, the plasma density is often as low as 1cm^{-3} in the higher magnetospheric orbits under consideration for this mission. Under these conditions, beam emission will cause the spacecraft to

rapidly charge to the beam potential and pull the beam back unless it is properly neutralized (as shown via simulation in figure 1).
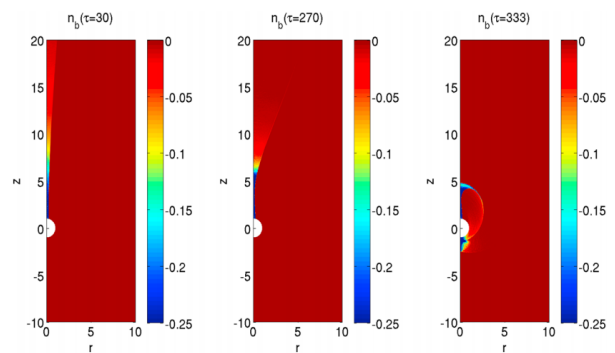

Figure 1. Simulation of electron beam emission and subsequent return without contactor plasma [1].

One proposed neutralization technique is ion emission from a hollow cathode generated plasma plume. Simulations suggest this technique is possible given sufficient hollow cathode discharge current and plasma plume expansion [3]. In this technique, the positive potential of the charged spacecraft repels ions from a dense plasma plume surrounding the spacecraft. These ions are emitted from the edge of the plume and leave the spacecraft system. Emission from the edge of the expansive plasma plume allows the ions to overcome the space-charge limit typical of ion beam emission [3].

The ion emission technique requires that the contactor current (calculated using the number of free ion-electron pairs ejected per second) be greater than the beam current. Simulations indicate that for smaller contactor currents, the spacecraft potential will reabsorb all ambient electrons and push away the surrounding ion cloud [3]. The underlying physics of this technique is not application specific and thus it may be used to neutralize a host of different charged objects. Other potential applications for hollow cathode based neutralization

include electrodynamic tether current enhancement, reduction of potential transient magnitude for rapid charging events (such as solar array unshunts), and reduction of high power electric propulsion system generated spacecraft charging.

2. EXPERIMENTAL SETUP

2. 1. "Spacecraft" Isolation Circuit

In order to mimic simulations and in-space conditions for a representative "spacecraft" (S/C), we must be able to electrically isolate it from conducting surfaces in contact with Earth ground. This was accomplished by placing all hollow cathode components on top of a conducting steel plate. This plate was separated from the steel chamber via four 6" ceramic standoff insulators (see figure 2). High voltage ceramic feedthroughs, coaxial and twisted pair cable arrangements, and woven metal shielding sleeves were used when possible.
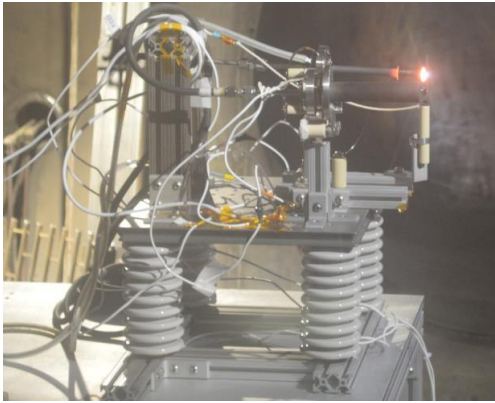

Figure 2. Simulated "spacecraft" with primary hollow cathode in operation.

Because hollow cathodes are an integrated part of the spacecraft, it is essential that all hollow cathode power supplies bias the cathode relative to the S/C potential. This means that as the S/C potential floats, the cathode and keeper potentials will adjust automatically and be held constant relative to this changing value rather than Earth ground. Thus the power supply "ground" or neutral line must be held at the S/C potential. A 1:1 isolation transformer was used to power these power supplies and disconnect their neutral line from Earth ground. This is possible because transformers couple voltages between windings via an oscillating magnetic flux according to Faraday's Law of Induction. The 60Hz AC wall voltage is able to couple between windings because it is sinusoidal. A DC potential difference between windings, however, generates no change in magnetic flux and thus the DC potential of the two windings can be completely independent. The use of this transformer effectively

severs the current path to ground via the hollow cathode power supplies.

A high voltage (20kV) power supply is used to simulate the electron beam for this first round of experiments. This power supply is grounded to provide it with some reference potential. It is used in both constant current and constant voltage mode to control the S/C potential. For transient testing in which the "beam" is fired, the power supply is simply switched on and off in constant current mode. The power supply's voltage and current is independently verified and recorded using an oscilloscope. The current is converted to a voltage using a simple, in-series, 1 Ohm resistor voltage drop (see figure 3 for the complete isolation circuit).
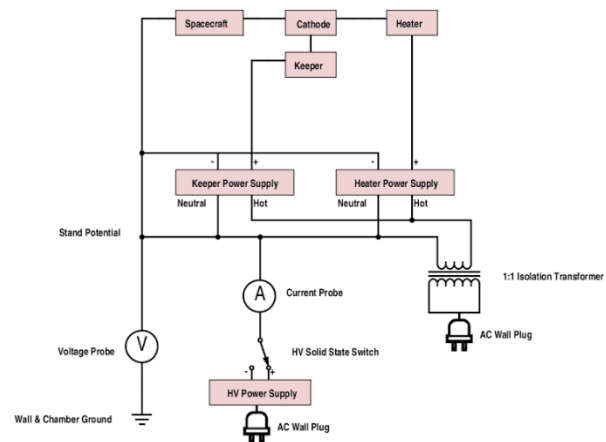

Figure 3. "Spacecraft" isolation and hollow cathode power supply circuit.

2. 2. Plasma Diagnostics

4 cylindrical Langmuir probes, an emissive probe, and an RPA were used over the course of these experiments. Excluding the two Langmuir probes placed 6cm from the chamber wall and 96cm behind the hollow cathode, the diagnostics were located on the diagnostic suite shown visually in figure 4. This diagnostic suite featured 2 large linear motion stages and a rotation stage. Probes were isolated and extended from the rotation stage to prevent wake effects and possible arcing to the chamber. This created a large effective testing area and placed probes at approximately the same height as the hollow cathode orifice (+/- 2cm).

The only probe measurements used in this analysis are those made by the emissive probe 206cm downstream of the hollow cathode orifice on centerline. These plasma potential measurements were made using the floating point with large emission method. In this method, a current is passed through the thin probe filament to heat it to electron emission temperatures. These electrons effectively neutralize the sheath around the filament so

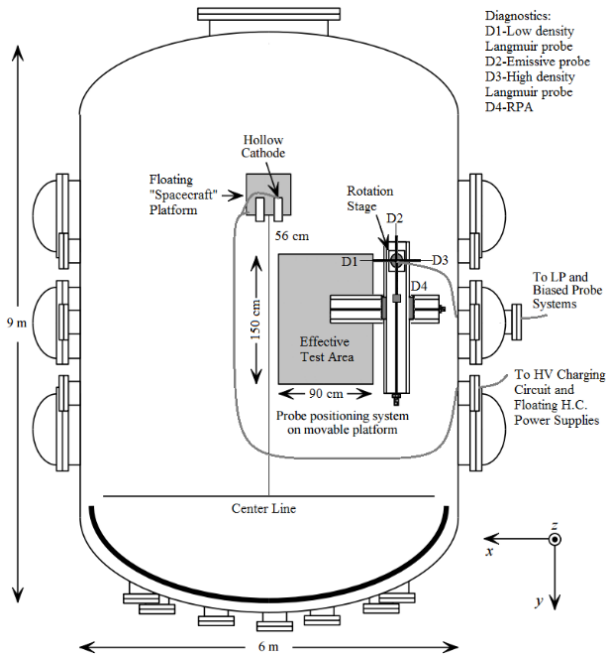that the probe floats very close to the plasma potential [4].

Figure 4. Aerial view of the LVTF Test Setup including diagnostic suite.

3. RESULTS

3. 1. S/C Potential Transient

Transients were taken once the hollow cathode had reached equilibrium at a gas flow rate of 7sccm, discharge current of 5A, and keeper potential of 26.6V. Figure 5 shows the current supplied by the high voltage power supply reaches its steady state value in approximately 255ms. The current was set to 33mA, but an analysis of figure 5 reveals the average current during the beam firing of 30.6mA. It is likely that the high voltage power supply was unable to set the current to e 33mA with a high degree of accuracy as it is well below its maximum current setting. Thus this 2.4mA discrepancy is likely within the uncertainty of the power supply. It is also important to note that the current measurement is rather noisy. This is likely because of the current measurement technique used. The cables and resistor were partially unshielded and in a control room with significant electromagnetic interference (EMI). This EMI could easily couple to the current sensing circuit and induce voltage on the order of a few mV, but would not alter the current's average value.
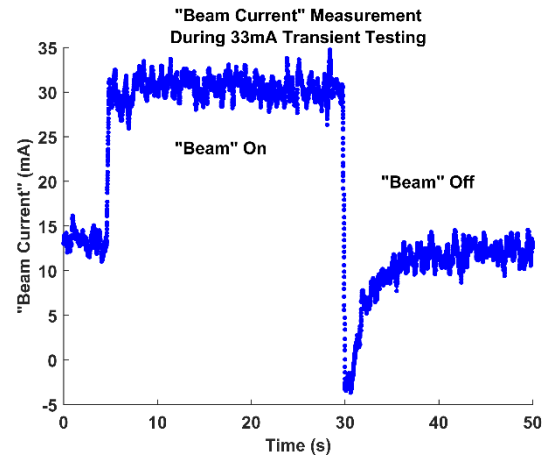

Figure 5. "Beam current" during 33mA transient testing filtered with a 50 point moving average.

Figure 5 indicates that the high voltage power supply used is capable of mimicking electron beam emission with the possible exception of its 255ms rise time. However, this rise time is insignificant in comparison with the time it takes for the S/C and plasma potentials to reach equilibrium. It is clear from figure 6 that it takes the system over 15 seconds to reach equilibrium. The S/C potential and plasma potential also change with no visible delay between their signals. The rapid initial rise time and lack of delay between potentials suggest that the plasma responds quickly to the "beam current" as one would expect from typical diffusion and plasma frequency time constants. This makes the long potential equilibrium time even more mysterious and possible causes of this phenomenon are presented in the discussion.
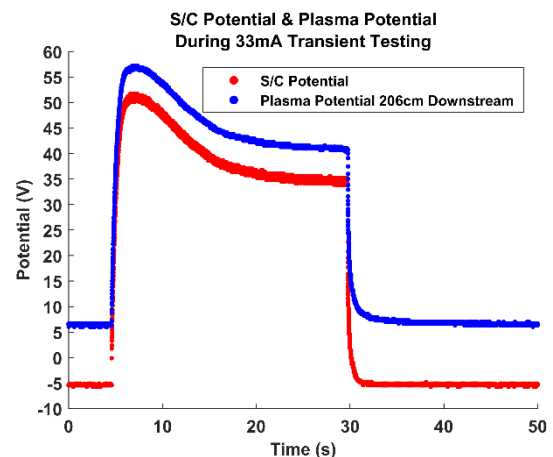

Figure 6. Potential transients during 33mA "beam" firing.

3. 2. Key Hollow Cathode Parameters

"Beam current" was varied and steady state S/C potential measured. As expected, the S/C charges to higher

potentials for higher beam currents as seen in figure 7. The S/C potential is negative for low beam currents to maintain the flux balance between collected electrons and ions (it floats slightly negative to repel the faster moving electrons).
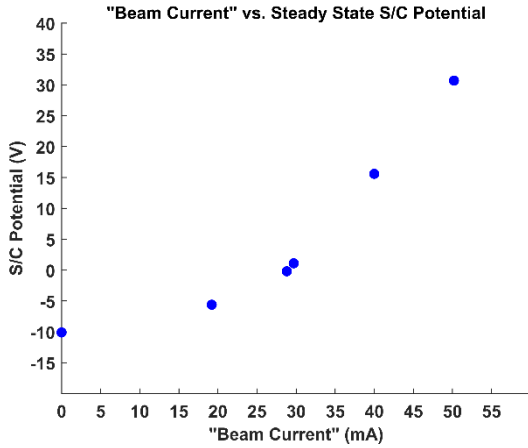

Figure 7. "Beam current" vs steady state S/C potential for a discharge current of 5A and flowrate of 7sccm.

The plasma potential 206cm downstream was also recorded for these conditions. In general, the plasma potential increases with the S/C potential as seen in figure 6. However, closer inspection reveals the relationship is not quite 1-to-1. The potential drop of the plasma potential relative to the keeper potential is summarized in figure 8. It is clear that the plasma potential drops off more over the same distance for higher S/C potentials. Accounting for this additional drop and linearizing the three highest S/C potential points, we find that the plasma potential 206cm downstream changes by roughly 77% of the S/C potential.
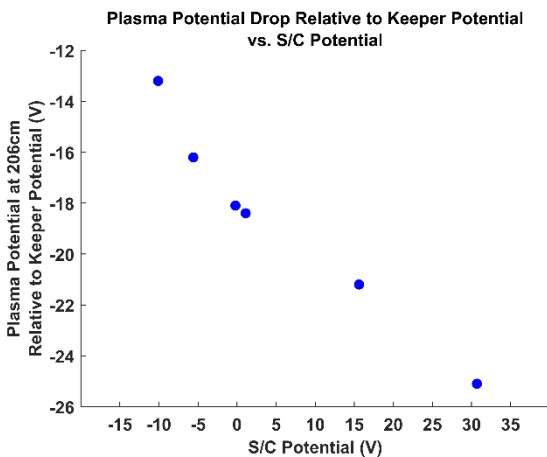

Figure 8. Plasma potential drop relative to keeper potential vs steady state S/C potential for a discharge current of 5A and flowrate of 7sccm.

One key hollow cathode parameter identified during the simulation efforts of [3] is the contactor current. Due to the coupled and complex nature of hollow cathodes, this value cannot be easily set or determined. However, one way to alter this value indirectly while maintaining the chamber pressure is to change the keeper discharge current. Increasing the keeper current has been shown to increase the hollow cathode ionization fraction (the percentage of injected neutral gas which is ionized by the hollow cathode) and thereby increase the contactor current in a roughly linear fashion [5,6]. Figure 9 presents the steady state S/C potential when varying the keeper current. It is clear that increasing the keeper/contactor current lowers the S/C potential and makes the hollow cathode a more effective neutralizer. Figure 9 shows the relationship is surprisingly linear, with the largest deviations occurring at extremum where deviation is to be expected.
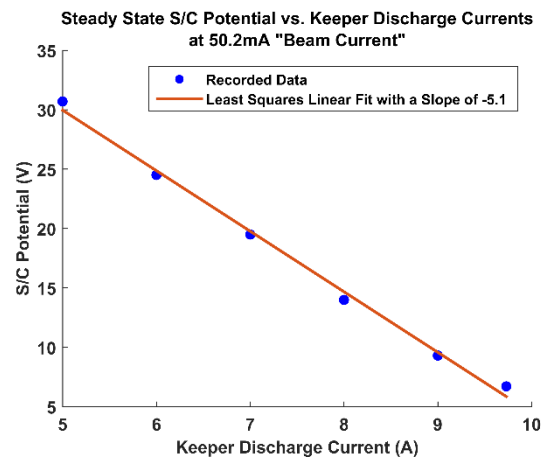

*Figure 9. Steady state S/C potential vs keeper current at 50.2mA "beam current" and a flowrate of 7sccm.*

Changing the keeper current has the added effect of changing the temperature of the hollow cathode as more power is dissipated as heat for higher keeper currents. This raises the question of whether the increase in neutralization effectiveness was caused by the increase in temperature or the increase in cathode current as predicted. The hollow cathode heater was used to explore this possibility. A 5A current was run through the heater in addition to a keeper current of 5A for a combined hollow cathode power similar to the 9A keeper current case. It was found that keeping keeper current constant and increasing the hollow cathode temperature actually decreased the neutralization effectiveness. The results of these tests are summarized in table 1 below.

Configuration	1	2	3
Keeper Current (A)	5	5	9
Heater Current (A)	0	5	0
Combined Cathode & Heater Power (W)	135	208	201
Beam Current (mA) SS S/C Potential = 0V	13.7	9.3	10.3
Beam Current (mA) SS S/C Potential = 30V	38.1	28.2	51.8
Beam Current (mA) SS S/C Potential = 60V	39.5	35.8	63.7

Table 1. Neutralized "beam current" for varying hollow cathode heating configurations.

3. 3. Microdischarges

Microdischarges were observed in the chamber when the S/C potential exceeded 60V. These microdischarges consisted of a small flash of light on a grounded chamber surface (see figure 10) and an almost instantaneous reduction of the S/C potential to Earth ground. The high voltage power supply also experienced a simultaneous current burst. Microdischarges occurred at seemingly random times under high S/C potential conditions, with their frequency increasing for higher S/C potentials. They also took place throughout the chamber, but were mostly concentrated near the simulated S/C and on the diagnostic suite when it was brought close to the hollow cathode orifice. Microdischarge frequency could be reduced by "conditioning", in which the S/C potential was raised over extended periods of time to "blast off" impurities and likely discharge points. While conditioning increased the maximum discharge-free S/C potential slightly, this was ultimately the limiting factor on maximum S/C potential during testing.
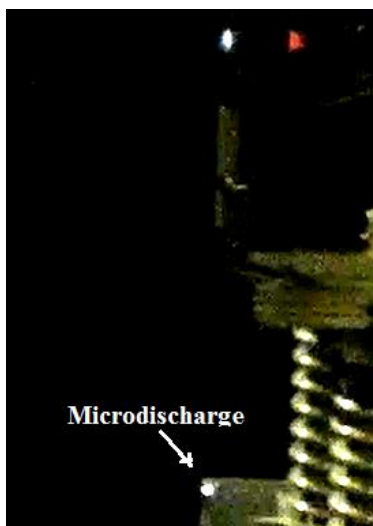
Microdischarge

(a.)

(b.)

Figure 10. Photos showing (a.) a microdischarge and (b.) microdischarge damage to a rough aluminum plate at the conclusion of testing.

4. DISCUSSION

One possible explanation for long S/C potential equilibrium times is thermal effects. The hollow cathode's thermal equilibrium is somewhat disturbed by the firing of the "beam" and thermal time scales can be on the order a few seconds in our physical system. The mean free path of Xenon symmetric charge exchange (CEX) collisions is also less than a meter for the relatively high pressure regions near the cathode orifice and a cross section on the order of $8*10^{-19}m^2$ [6,7]. This would indicate that the majority of Xenon ions charge exchange with neutral Xenon atoms before leaving this region, as explained in [8]. When the beam is fired and the S/C charges, there is suddenly a larger electric field accelerating ions out of the keeper orifice (see figure 8). This increase in ion energy could then slowly be transferred to neutral gas heating via CEX collisions. Once the system has again achieved thermal equilibrium, the ion energy/diffusion is again maximized and the gas temperature/mobility increased.

Pumping effects caused by the residual gas time in the chamber could also contribute to long equilibrium time scales. Chamber cryopumps act to maintain a constant pressure. If the gas temperature were to increase, the pressure would also increase and pumps would act to reduce the chamber neutral density. For a plasma dominated by ambipolar diffusion and limited by CEX collisions such as those within and near the hollow cathode orifice, the ambipolar diffusion coefficient is given by Eq. 1 below [6].

$$D_a = \frac{e}{M} \frac{(T_i(eV) + T_e(eV))}{\sigma_{CEX} n_0 v_{scat}} \qquad v_{scat} = \left(\frac{kT_i}{M}\right)^{\frac{1}{2}} \qquad (1)$$

D_a is the ambipolar diffusion coefficient, e is the fundamental charge, M is the ion mass, T_i and T_e are the ion and electron temperature respectively, k is

Boltzmann's constant, n_0 is the neutral density, σ_{CEX} is the charge exchange cross section, and v_{scat} is the ion thermal speed. Although the results are not presented in this paper, T_i and T_e increased when the beam was being fired as expected [9]. These changes likely occurred quickly in response to the S/C potential. The change in n_0 is less dramatic and requires more time and thus may account for the long equilibrium time as the diffusion rate ultimately determines the neutralization effectiveness.

Capacitive effects are the final possible contributor to long equilibrium times discussed in this paper. Potential transients of a similar shape have been observed on geosynchronous satellites operating a neutralizer (such as ATS-5) [10]. Replication of the ATS-5 mission via NASCAP simulation reveals that differential charging and large capacitances between spacecraft surfaces drive long equilibrium times [10]. Using a simple series RC circuit, we can approximate our plasma resistance by linearizing the last three points of figure 7 (for a resistance of roughly 1450Ω). An approximate S/C to chamber wall capacitance can be produced by treating the isolated conducting plates as a parallel plate capacitor whose separation is the isolation ceramic height (this results in a capacitance of 68.1pF). The simulation current source can be modeled after the power supply current shown in figure 5. Figure 11 summarizes the S/C potential transient simulation results using Keysight's ADS software. It is interesting to note that the magnitude and time scale of this capacitive effect are very similar to those observed in figure 6.
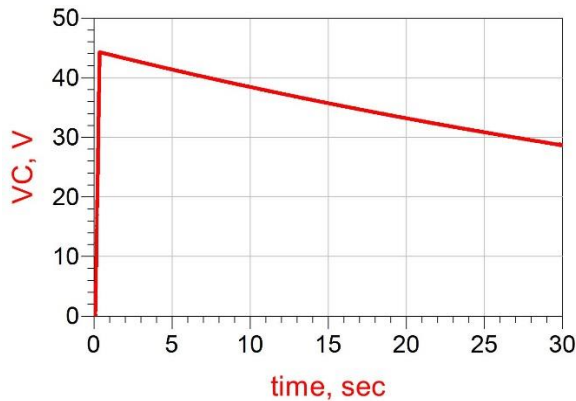

Figure 11. Capacitive charging transient simulation using basic series circuit model.

The ion emission technique requires that the contactor current be greater than the beam current. For the 7sccm Xenon flowrate used, the maximum contactor current is 0.5A for a 100% ionization fraction. Hollow cathodes typically have an ionization fraction in the 10-50% range [5]. The maximum "beam current" presented in this paper (50.2mA) thus corresponds to an ionization

fraction of 10.4% and we can assume measurements were made using the ion emission technique. It is interesting to note that microdischarges first began to occur just above a "beam current" of 50.2mA. It is possible that the ionization fraction of this hollow cathode is between 10 and 20 percent for a keeper current of 5A and increasing the "beam current" beyond 50.2mA violates the beam current < contactor current requirement. If this is the case the S/C and plasma potentials would rise rapidly and could spark microdischarges.

Microdischarges are potential dependent events in which a region of neutral gas is briefly ionized. Because they occurred on chamber surfaces where the sheath potential was largest, we can assume that microdischarges were started by ions traversing the sheath and striking the chamber surface with energy exceeding 50eV. It is possible that microdischarges occur once the secondary electron yield (SEY) of incident ions surpasses some critical value. Indeed, the SEY of this system increases for higher potentials [11]. If the local neutral density is also sufficiently high (possibly enhanced by material sputtered off the chamber surface), a corona discharge may be initiated as electrons are accelerated to energies exceeding Xenon's ionization threshold (12.1eV) [6]. This burst of charged particles then quickly reduces the S/C potential, exhausts the sputtered material, and extinguishes itself.

5. CONCLUSIONS

Ion emission using a hollow cathode appears to be a viable neutralization technique. It successfully prevented the S/C potential from increasing without bound and equilibrium was achieved at some relatively small positive value. Contactor current is clearly a critical parameter as predicted by theory, while the hollow cathode temperature appears to be less important. Additional tests and analysis will be needed to explore the cause of long potential equilibrium times when the beam is fired. Microdischarges present a relatively low upper limit on testing potentials, however it may be possible to reduce their frequency by adjusting the experimental setup.

REFERENCES

1. Delzanno, G.L., Borovsky, J.E., Thomsen, M.F., Moulton, J.D., & MacDonald, E.A. (2015). Future beam experiments in the magnetosphere with plasma contactors: How do we get the charge off the spacecraft?, J. Geophs. Res., 120(5), 3647-3664.
2. Winckler, J. R. (1980). The Application of Artificial

Electron Beams to Magnetospheric Research, Rev. Geophs. & Space Physics, 18(3), 659-682.

3. Delzanno, G.L., Borovsky, J.E., Thomsen, M.F., & Moulton, J.D. (2015). Future beam experiments in the magnetosphere with plasma contactors: The electron collection and ion emission routes, J. Geophs. Res., 120(5), 3588-3602.

4. Sheehan, J.P. & Hershkowitz, N. (2011) Emissive Probes, Plasma Sources Sc. Technol., 20.

5. Goebel, D.M., Jameson, K.K., Katz, I. & Mikellides, I.G. (2007). Potential fluctuations and energetic ion production in hollow cathodes discharges, Phys. Plasmas, 14.

6. Goebel, D.M. & Katz, I. (2008). Fundamentals of Electric Propulsion: Ion and Hall Thrusters, JPL Space Science and Technology Series.

7. Miller, J.S., Pullins, S.H., Levandier, D.J., Chiu, Y.H. & Dressler, R.A. (2002). Xenon charge exchange cross sections for electrostatic thrusters models, J. Applied Physics, 91(3), 984-991.

8. Sasaki, S., Kawashima, N., Kuriki, K., Yanagisawa, M., & Obayashi, T. (1987). Neutralization of Beam-Emitting Spacecraft by Plasma Injection, J. Spacecraft, 24(3), 227-231.

9. Leon, O., Miars, G., Gilchrist, B., Delzanno, G.L. & Borovsky, J. (2016). Plasma Plume Behavior in the Presence of Biased Spacecraft. SCTC 2016.

10. Olsen, R.C. (1985) Experiments in Charge Control at Geosynchronous Orbit – ATS-5 and ATS-6. J. Spacecraft, 22(3)

11. Maric, D., Savic, M., Sivos, J., Skoro, N., Radmilovic-Radjenovic, M., Malovic, G. & Petrovic, Z.L. (2014) Gas breakdown and secondary electron yields. Eur. Phys. J. D., 68(155).